because the cross section of fission and absorption in that region for fissile materials such as $^{235}U$ and $^{239}Pu$ are enormous. Previous study[1] has shown that 69-group cross sections created by ENDF/B-VI and LEAPR, which create the $S(\alpha,\beta)$ scattering law for incoherent scatters, matched very well with other benchmark results such as Ref. 2. The transport code used in that study was TWODANT. In this study, another approach to benchmarking temperature feedback coefficients is attempted by using a Monte Carlo transport code, MCNP.

## CALCULATION OF TEMPERATURE FEEDBACK COEFFICIENT

MCNP is a Monte Carlo code with various purposes in nuclear system. Because MCNP uses a continuous-energy spectrum, it takes the low hydrogen scattering effect such as the $S(\alpha,\beta)$ scattering law into the calculation as well. Studying the change of multiplication $k$ over a temperature range is necessary to see whether it is possible to calculate temperature coefficients using this type of code. Figure 1 gives the results of the study using 95% enriched $^{239}Pu$ in a 400 g/ℓ water solution. Although the trend is clearly linear, we do see some fluctuation of $k$ values due to the nature of a Monte Carlo code. By picking two $k$ values at two different temperature settings, reactivity feedback due to the change in temperature can be studied.

## TEMPERATURE COEFFICIENTS OF PLUTONIUM SOLUTION

Temperature feedback coefficients are calculated for different regions of plutonium concentration in water. From previous work done by Kornreich[1] and Mather et al.,[2] it has been shown that in low concentrations of plutonium in solution, positive temperature feedback coefficients can take place. Figure 2 is the graph comparing Kornreich's temperature coefficient calculation by the TWODANT code with a 69-group cross section and those from MCNP with continuous-energy spectrum. As seen in the graph, the results from the MCNP code and TWODANT for temperature feedback agree very well with each other.

## CONCLUSION

This study has been done to benchmark the results from the MCNP code with continuous-energy spectrum against the results from the TWODANT code. The results from the TWODANT code have been validated in a previous work,[1] and the results from MCNP matched very well with the TWODANT code, showing that MCNP can be reliably used to calculate temperature feedback coefficients in a nuclear system.

1. E. D. KORNREICH, "Reactivity Feedback Mechanisms in Aqueous Fissile Solutions," MS Thesis, University of Arizona (1992).

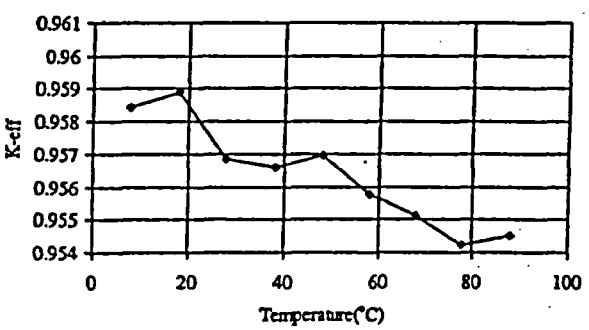


Fig. 1. Temperature versus $k_{eff}$ value.

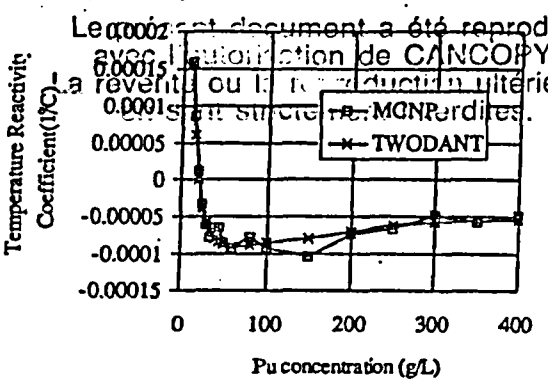


Fig. 2. Comparison of temperature feedback coefficients.

2. D. J. MATHER, A. BICKLEY, A. PRESCOTT, F. BARBRY, J. P. ROZAIN, P. FOUILLAUD, "Examination of Some Fissile Solution Scenarios Using CRITEX," presented at Int. Conf. Nuclear Criticality Safety, Oxford, England (1991).

## 5. Validation of MCNP4A for $UO_2$-$ThO_2$ Systems in Water, *Scott M. Revolinski, Debdas Biswas (Westinghouse SRC)*

The Receiving Basin for Offsite Fuel (RBOF) at the Savannah River Site is a facility for receipt and storage of many varieties of spent nuclear fuels from off-site reactors. The purpose of this paper is to validate MCNP4A with the ENDF/B-V pointwise cross-section set with two sets of critical experiments using $UO_2$-$ThO_2$ fuel rods in water and thereby develop a bias for use in the nuclear criticality safety studies involving Elk River Reactor (ERR) and Dresden fuels (also containing $UO_2$-$ThO_2$) stored in RBOF. Five Thorium Uranium Physics Experiments (TUPE), as documented in the Babcock & Wilcox (BAW-1191) report, and five Consolidated Edison Thorium Reactor (CETR) Criticals, as documented in the Babcock & Wilcox (BAW-119, Rev. 1) report, are identified as having the constituents desired for this validation as well as sufficient experimental details to allow accurate construction of MCNP4A calculation models. The validation has been performed on IBM RISC 6000 machines with the configuration-controlled version of the MCNP4A code. Of particular interest is an evaluation of the state of ENDF/B-V $^{232}Th$ cross-section data for criticality safety studies.

## CRITICAL EXPERIMENTS

The TUPE experiments utilized a uniform lattice core containing thorium-oxide uranium-oxide fuel pins clad with aluminum in water. The metal-to-water volume ratio varied from 0.3 to 1.0. The five TUPE experiments considered for validation used two types of fuel pins, namely, 15/1 and 25/1, corresponding to $^{232}Th/^{235}U$ atom ratios of 15 and 25.34, respectively. The densities for 15/1 and 25/1 fuel pins are 8.35 and 8.45 g/cm$^3$, respectively, and the enrichment is ~93%. The pins were loaded in a core tank on a square pitch and held in place by two egg-crate grids, one placed on a 10.16-cm-thick aluminum plate at the bottom of the tank, the other held by an aluminum structure ~152 cm above the bottom structure. The cores were clean, and no control or safety rods were inserted. The water levels were adjusted for criticality.

The CETR experiments also used uniform lattice and $UO_2$-$ThO_2$ pins clad with Type 304 stainless steel in water. The metal-to-water volume ratio was near 1.0. No control or safety rods were inserted. Fuel pins were loaded on a square pitch for

**TABLE I**

**Summary of TUPE and CETR Cores**

| Parameters | TUPE-7 | TUPE-7 | TUPE-7 | TUPE-4 | TUPE-4 |
|---|---|---|---|---|---|
| | 15A | 15B | 15D | 25√2B | 25D |
| Pin Type | 15/1 | 15/1 | 15/1 | 25/1 | 25/1 |
| Pellet, OD (cm) | 0.660 | 0.660 | 0.660 | 0.594 | 0.594 |
| Clad Thickness (cm) | 0.03556 | 0.03556 | 0.03556 | 0.08636 | 0.08636 |
| Pin, OD (cm) | 0.785 | 0.785 | 0.785 | 0.785 | 0.785 |
| Clad Material | Al | Al | Al | Al | Al |
| Active Pin Length (cm) | 152.4 | 152.4 | 152.4 | 152.4 | 152.4 |
| Total Pin Length (cm) | 157.01 | 157.01 | 157.01 | 157.01 | 157.01 |
| Pin Pitch (cm) | 0.978 | 1.023 | 1.222 | 1.446 | 1.222 |
| Total Number of Pins | 1108 | 880 | 514 | 1146 | 1176 |
| Equivalent Core Radius (cm) | 18.37 | 17.12 | 15.63 | 27.3 | 23.6 |
| Critical Water Height (cm) | 127.21 | 133.44 | 135.0 | 135.3 | 140.5 |
| H/U-235 Ratio | 77.9 | 92.8 | 166.5 | 540.3 | 338.9 |
| Pellet Atom Densities : | | | | | |
| U-235 (a/b-cm) | 0.118193E-2 | same as 15A | same as 15A | 0.729064E-3 | same as 25√2B |
| U-238 (a/b-cm) | 0.690684E-4 | | | 0.545795E-4 | |
| Th-232 (a/b-cm) | 0.177261E-1 | | | 0.184664E-1 | |
| O (a/b-cm) | 0.385455E-1 | | | 0.376128E-1 | |
| [illegible] | [illegible] | [illegible] | [illegible] | [illegible] | [illegible] |
| | CETR 7A | CETR 7B | CETR 9A | CETR 9B | Single Zone |
| Pin Type | 25/1 | 25/1 | 15/1 | 15/1 | 15/1 |
| Pellet, OD (cm) | 0.660 | 0.660 | 0.660 | 0.660 | 0.660 |
| Clad Thickness (cm) | 0.03556 | 0.03556 | 0.03556 | 0.03556 | 0.03556 |
| Pin, OD (cm) | 0.792 | 0.792 | 0.792 | 0.792 | 0.792 |
| Clad Material | SS | SS | SS | SS | SS |
| Active Pin Length (cm) | 121.92 | 121.92 | 121.92 | 121.92 | 121.92 |
| Total Pin Length (cm) | 127.0 | 127.0 | 127.0 | 127.0 | 127.0 |
| Pin Pitch (cm) | 1.02286 | 0.9665 | 1.02286 | 0.9665 | 0.9665 |
| Total Number of Pins | 4465 | 6529 | 1331 | 1771 | 1576 |
| Equivalent Core Radius (cm) | 40.5 | 44.9 | 22.3 | 24.2 | 25.9 |
| H/U-235 Ratio | 152.1 | 121.2 | 91.2 | 72.7 | 72.7 |
| Pellet Atom Densities : | | | | | |
| U-235 (a/b-cm) | 0.72284E-3 | same as 7A | 0.11819E-2 | same as 9A | same as 9A |
| U-238 (a/b-cm) | 0.54129E-4 | | 0.69068E-4 | | |
| Th-232 (a/b-cm) | 0.18311E-1 | | 0.17726E-1 | | |
| O (a/b-cm) | 0.37296E-1 | | 0.38546E-1 | | |

the first four experiments, and they were held in place by two aluminum grids. The fifth experiment consists of a single zone, where the pins were loaded into square aluminum cans, and the cans were placed into a lattice. Table I gives all pertinent details of fuel pins and lattices of the TUPE and CETR cores.

## MCNP MODELS AND ASSUMPTIONS

All MCNP4A models of the critical experiments are explicit, thus minimizing assumptions and approximations. Both TUPE and CETR experiments are well documented. However, some assumptions are used to build MCNP4A models, as noted next.

The core tank containing the fuel pins is not modeled. Instead, 30 cm of water is placed radially around the active core region. The top and bottom fittings of the fuel pins and the bottom support plate are accurately modeled, but there is no information beyond the 10-cm bottom support plate. Therefore, void is assumed below the support plate. There are no explicit values for critical water heights for any of the CETR experiments. It is stated that all pins are fully submerged. The exact locations of the empty safety rod channels are not specified in the CETR cores, and they are determined from a photograph. The impurities are specified for 15/1 fuel pins only and are modeled explicitly, but their effect on $k_{eff}$ is found to be negligible.

## RESULTS

The MCNP4A values for $k_{eff}$ from the covariance-weighted combined estimator and the corresponding standard deviations for each of the ten critical experiments are presented in Table II. The MCNP4A calculations used 1500 neutron/cycle for 160 cycles and skipped 50 initial cycles in each case.

The average value of $k_{eff}$ for the ten critical experiments is 1.005. All results agree with the experimental critical values within 1.5%. The overall distribution with ten data points looks normal using the Shapiro-Wilk test for normality. But a slight trend, an increase in $k_{eff}$ when the hydrogen/$^{235}$U ratio increases, is observed for TUPE cores. It is noted that the spread of hydrogen/$^{235}$U ratios is large in the TUPE cores compared with those in the CETR cores. The total experimen-

TABLE II

TUPE and CETR $k_{eff}$

| Critical Experiments | H/U-235 | MCNP4A Calculated $k_{eff}$ ± σ | Experimental $k_{eff}$ |
|---|---|---|---|
| TUPE 15A | 77.9 | 0.9968 ± 0.0019 | 1.0000 |
| TUPE 15B | 92.8 | 0.9988 ± 0.0017 | 1.0000 |
| TUPE 15D | 166.5 | 1.0104 ± 0.0018 | 1.0000 |
| TUPE 25√2B | 540.3 | 1.0142 ± 0.0015 | 1.0000 |
| TUPE 25D | 338.9 | 1.0136 ± 0.0013 | 1.0007 |
| CETR 7A | 152.1 | 1.0003 ± 0.0015 | 1.0005 |
| CETR 7B | 121.2 | 1.0015 ± 0.0015 | 1.0006 |
| CETR 9A | 91.2 | 0.9988 ± 0.0017 | 1.0004 |
| CETR 9B | 72.7 | 1.0143 ± 0.0017 | 1.0002 |
| CETR Single Zone | 72.7 | 1.0010 ± 0.0016 | 1.0000 |

tal accuracy was quoted as better than 2%. All calculated $k_{eff}$ values are greater than one, except for three experiments. A 95/95 single-sided lower tolerance limit for normal distribution is calculated to be 0.943, using all calculated $k_{eff}$ numbers.

The TUPE and CETR MCNP4A results appear consistent for a wide range of moderation and fuel lattices. It is shown that MCNP4A with an ENDF/B-V cross-section set can accurately and conservatively model uranium-thorium systems in water. With some additional sensitivity studies, these experiments may be included in the international handbook of critical experiments to calculate bias for uranium-thorium systems.

## 6. Criticality Evacuation Detectors That Locate the Accident Site, *J. T. Mihalczo, D. P. Hutchinson, J. A. Williams, L. H. Thacker (ORNL)*

Currently, criticality evacuation alarms[1] are dispersed in nuclear processing facilities to alarm when a criticality accident has occurred. They are spaced to provide adequate coverage of a nuclear process area with a minimum number of detectors. Several alarms can trip simultaneously from the same criticality excursion. For example, prompt critical excursion experiments with the Health Physics Research Reactor in the Critical Experiments Facility (CEF) of the Oak Ridge Y-12 plant in 1961 tripped several criticality evacuation alarms in the main part of the Y-12 plant, which was separated from the CEF by a considerable distance and an ~200-ft hill. Current alarm systems provide little information on the specific location of a criticality accident within a building. As a result, not knowing the exact location of a criticality excursion can lead to evacuation paths that do not minimize radiation exposure.

The system proposed here employs a scintillation-based detector array or, alternately, a pin silicon diode array coupled with analysis electronics designed to not only produce an evacuation alarm but to determine the exact site of the criticality event so that optimum (lowest dose) evacuation paths can be determined instantaneously and automatically and can be quickly displayed for personnel evacuation. This system would also store the dose and time data comparison during and after the accident so that the information can be used for postaccident analysis.

The system described here utilizes a large number of inexpensive detectors dispersed on a regular grid throughout a processing facility (say, on the ceiling). These detectors are input to a system that localizes the criticality accident and instantaneously determines and displays optimum paths for minimum exposure for personnel evacuation. These paths would be displayed by systems of arrows throughout the facility that display the evacuation route.

A wide variety of reliable, inexpensive radiation detectors for monitoring stored special nuclear materials has been developed for the continuous automated vault inventory system (CAVIS) at the Oak Ridge Y-12 plant.[2] These detectors, with the sensitivity adjusted for this application, make this concept feasible. For example, one type of CAVIS detector is a self-powered scintillation detector coupled to a fiber-optic cable for transmission of the light to processing stations,[3] which record the radiation level above the trip point as a function of time. A schematic diagram of a gamma-ray probe based on a commercially available plastic scintillator (less than $50, including electronics) is shown in Fig. 1. This type of detector has the advantage that there are no active circuits in the processing area, just passive, self-powered scintillation detectors coupled to fiber-optic cables.

The ~420-nm scintillation light is absorbed in wavelength shifting fibers (WSFs) mechanically coupled to the probes and re-emitted at a wavelength of ~500-nm. The WSFs are heat bonded to clear fibers that transmit the shifted light without significant attenuation over distances >100 m to either multianode photomultiplier tubes or arrays of solid-state photodetectors. The probes are covered with a light-tight, environmentally rugged rubberized coating.

Fiber-coupled scintillation probes have been developed that may be constructed to be sensitive either to neutrons or gamma